Effects of hyperoxia on retinal autophagy in a mouse model of retinopathy of prematurity

Jie Wang
the first affiliated hospital of zhejiang chinese medicion university
Ergang Du
the first affiliated hospital of zhejiang chinese medicine university
Yunliang Zheng (ylzheng1984@zju.edu.cn)
Durg evaluation

Research article

Keywords: Retinopathy of prematurity, Autophagy, Retina, Hyperoxia

Posted Date: December 18th, 2019

DOI: https://doi.org/10.21203/rs.2.19175/v1

Abstract

Purpose

To evaluate the autophagy activation of retina in an oxygen-induced retinopathy of prematurity (ROP) mouse model.

Methods

C57BL/6 mice were exposed to 75 ± 0.5% oxygen from P7 to P12, after which they were brought into room air and raised to P17. Mice underwent fluorescein angiography of the retinal vasculature on P17. The thickness and ultrastructural of retina was observed on P17. The expression of autophagy in the retina tissue was assessed by Quantitative real-time polymerase chain reaction and Western blot analysis.

Results

The neovascularization was significantly higher in the oxygen-induced mice. The retinal thickness of the oxygen-exposed group was higher than that of the control group on P17. The autophagosomes in retina of ROP mouse were observed. During the hyperoxia stage (from P8 to P13), the mRNA levels of Beclin1 (mammalian Atg6), Uncoordinated-51 like kinase 1 (ULK1), and Autophagy 5 (Atg5) were increased. At the relative hypoxia stage (raised in room air from P14 to P17), the expression of Beclin1, ULK1, and Atg5 mRNA levels was downregulated in retinas of ROP mice compare to the controls. Over time, the protein expression of Beclin-1, ULK1, and Bcl-2-associated X protein (Bax) was upregulated, but the protein expression of B-cell lymphoma 2 (Bcl-2) was downregulated.

Conclusions

Hyperoxia and relative hypoxia not only cause retinal neovascularization, but also change the autophagy markers in the retina of newborn mice.

Background

Retinopathy of prematurity (ROP), which afflicts infants born before term, is caused by oxygen-induced damage to the developing retinal vasculature [1]. Exposing the developing vasculature to hyperoxia causes the cessation of growth of retinal blood vessels, with their subsequent constriction and death [2]. Conventional therapies for ROP are limited to removing vasculature by surgery or intra-vitreal injection of anti-vascular endothelial growth factors (anti-VEGF) antibody [3]. However, the vision of ROP patients over the long term is still poor, and effective treatments for their blinding disorders are lacking. Previous research has indicated that photoreceptor and post-receptor responses are significantly altered years after the preterm days [4, 5], which means that not only is normal retinal vascularization disrupted, but the retinal cells are also damaged.

Autophagy is an intracellular pathway in which cytoplasmic constituents are delivered to the lysosomal pathway for degradation [6]. When cells are subjected to stress, such as hypoxia, injury, or starvation, autophagy is activated immediately (induced autophagy) [7]. Under mild stress, autophagic activity is beneficial for cell survival, while severe stress leads to dysregulated autophagy, which results in massive cell death. Thus, autophagy acts as a “double-edged sword” in cell survival. Recent studies have shown autophagy is involved in photoreceptor survival and death in other diseases [6, 8]. Autophagy increases in the retinas of diabetic patients; the loss of vision is associated with defects in autophagy [9]. At present, few studies have addressed autophagy mechanisms in ROP models. The knowledge of basic autophagy function in retinas of ROP patients is still limited. In this study, we examine the autophagy gene and protein in the retinas of an ROP model to further understand how autophagy maintains retinal function in ROP patients.

Methods

Animals

A total of 130 newborn C57BL/6 mice (Purchased from Shanghai SLAC Laboratory Animal Co.,Ltd) were used in the current study. All animal protocols were reviewed and approved by the institutional animal care committee of Zhejiang Chinese Medicine University and in accordance with the Association for Research in Vision and Ophthalmology statement for the use of animals in ophthalmic and vision research.

Experimental protocol

The mouse ROP model was established by Smith et al [10]. Briefly, mice were placed into an oxygen-enrichment device (Hangzhou APU Instrument and Equipment Co., Ltd.) at postnatal day of life 7 (P7) with their nursing mothers. In the device, mice were exposed to 75 ± 0.5% O_2 for 5 days (through P12), then were returned to room air and raised to 17 days (P17). Control animals were raised in normal room air for 17 days. Mice were further divided into a control group (n = 75) and an oxygen-exposed group (n = 75). Mice in both groups were supplied with standard mouse water and chow. Temperature and humidity were maintained at 25 °C and 75–80%, respectively. Day/light cycles of 12 hours were used. After the experiment, all mice were killed with carbon dioxide. The mice were placed in the container and carbon dioxide was injected into the container until the mice died.

Fluorescein Dextran Perfusion of the Retinal Blood Vessels

To observe the retinal vascular pattern, the perfusion in six mice (P17) was performed using fluorescein-conjugated dextran (MW = 2,000,000, Sigma, St. Louis, MO, USA) in phosphate buffered saline (PBS) [11, 12]. After injecting chloral hydrate in abdomen, the left ventricle of the heart was perfused with 0.3 mL fluorescein-conjugated dextran (50 mg / ml in 4% PBS). When the color of the mouse's lips turned yellow,

the eyeballs were enucleated immediately and then placed in 4% paraformaldehyde for 3 h. The retina was removed and four radial cuts were performed to flatten the retina under a surgical microscope. The flat-mounted retinals were viewed and photographed by a Zeiss LSM 880 confocal laser scanning microscope (Carl Zeiss, Oberkochen, Germany).

Hematoxylin and eosin (H&E)

On P17, 12 eyes of oxygen-exposed and control group mice were fixed immediately in 1% formaldehyde and 1.25% glutaraldehyde after enucleation for 48 h. Then, they were embedded in Optimum Cutting Temperature compound. Serial sections (5 μm thick) were cut through the cornea, parallel to the optic disc in a sagittal plane. The tissue sections were stained with hematoxylin and eosin (H&E). Under light microscopy, we observed the nuclei of the vascular endothelial cells of the neovascular vessels extending beyond the inner limiting membrane of the retina into the vitreal space, and we observed the thickness of retinal layers, as described by Smith and colleagues.[10]

Electron microscopy

Eyes of oxygen-exposed (four eyes) and control group (four eyes) mice were enucleated and fixed immediately in 2% glutaraldehyde and 4% paraformaldehyde on P17. Then the retinas were dissected and post-fixed in 2% aqueous osmium tetroxide for 1.5 h. After embedding in Epon, ultra-thin sections were cut at 1 μm and stained in uranyl acetate. The ultrastructures of retinal cells were observed under an electron microscope (Type 1400plus, Tokyo, Japan).

Quantitative real-time polymerase chain reaction (RT-qPCR)

Sixty eyes in each group, there are 10 time points, 6 eyes at each time point. Retinas from oxygen-exposed eyes and control eyes were dissected from the retinal pigment epithelial (RPE)-choroid at different time points (P8–P17). Total RNA of retinas was extracted using Trizol Reagent (Invitrogen, USA). Complementary DNAs (cDNAs) were synthesized with 4 μg of total RNA, according to the manufacturer's protocol for the Reverse Transcription Kit (TaKaRa, Japan). Based on the sequences reported in the GenBank database (Beclin-1: 5'-ggaccaggaggaagctcagtacc-3',5'-cgctgtgccagatgtggaagg-3';ULK1:5'-cggaccaggcagacattgagaac-3',5'-aggttggcagcaggtagtcagg-3';Atg-5:5'-gcaagccaaggaggagaagattcc-3',5'-gtgtctcagagaagcagtggtg-3'; β-actin:5'- gtgctatgttgctctagacttcg-3',5'-atgccacaggattccatacc-3'.), Beclin1 (mammalian Atg6), Uncoordinated-51 like kinase 1 (ULK1), and Autophagy 5 (Atg5), and β-actin primers were designed, selected, and ordered from Sangon (China). Quantitative real-time polymerase chain reaction (RT-qPCR) was performed with an ABI StepOnePlus Real-Time PCR System (Applied Biosystems, Foster City, CA, USA). A typical reaction was performed in 20 μL, consisting of 1 μL cDNA, 10 μL 2 × SYBR Green PCR buffer, and primer pairs (final volume 20 μmol each). The PCR temperature cycle was performed for 3 min at 95.0 °C, followed by 48 cycles with primer annealing for 30 seconds at 60.0 °C,

and extension for 30 seconds at 55.0 °C. ΔCT was calculated by subtracting the average threshold cycle (CT) of β-actin mRNA from the average CT of the target genes. All experiments were performed in duplicate. The comparative quantification values were obtained from the CT number at which the increase in signal was associated with an exponential growth of PCR products.

Western blot analysis

Total protein extract of retinas was obtained from mice eyes at P8–P17 (54 eyes in oxygen-exposed group and 54 eyes in control group), and protein concentrations were measured using a BCA Protein Assay kit (Beyotime, China). Samples containing 50 μg of protein were subjected to SDS-polyacrylamide gel electrophoresis gels (PAGE) using 10% and 15% polyacrylamide gel, then transferred onto a polyvinylidene difluoride membrane (Bio-Rad, USA). The membrane was blocked in 5% TBSA (10 mM Tris; pH 8.0, 150 mM NaCl, 0.5% Tween 20 and 5% fat-free dry milk) for 1 h at room temperature, then probed overnight at 4 °C with specific primary antibodies against Beclin-1, ULK1, Atg5, Bax, Bcl-2, and β-actin (1:1000; Cell Signaling Technology, USA), and incubated in blocking buffer with β-actin as an internal control. Immunoblots were then washed and incubated with a horseradish peroxidase-conjugated secondary antibody (Cell Signaling Technology, USA). Membranes were developed with the ECL substrate (Pierce, Thermo Scientific, USA). Images of labeled specimens were obtained with a ChemiDoc XRS imageing system (Bio-Rad Laboratories). Quantitation of bands were performed by densitometry using the Image Lab software (Bio-Rad Laboratories) and normalized to the expression of β-actin.

Statistics

Statistical analyses were performed using SPSS 18 (SPSS Inc., Chicago, IL, USA). Each group of animals was studied as an independent unit of analysis. Student's independent t-test was used to determine the significance of differences between the groups. Statistical significance was defined as a p value < 0.05.

Results

Effect of hyperoxygen on retinal vessels of ROP model

The results of the evaluation of the mounted retinas after fluorescein-conjugated dextran perfusion of the retinal blood vessels are presented in Fig. 1. Three mice lived in room air, retinal vessels were normal (Fig. 1A). Oxygen-exposed eyes displayed defects in vascular growth from the retinal periphery to the optic disc (Fig. 1B), and retinal periphery blood vessels are cluttered together (Fig. 1C). Hypoperfusion of blood vessels appeared around optic disc (Fig. 1D). There is a large number of neovascularization clusters in peripheral retina. .

Thicknesses of retinas in the ROP model were greater than in the control

Compared with mice raised in room air, the structures of retinas in ROP mice were altered. We observed the preretinal layers and thickness of retinas in the two groups at P17. Retinal structures appear normal in the room air group (Fig. 2A). The oxygen-exposed mice retinas showed edematous changes (Fig. 2B). The vessels protruded into the vitreous at the preretinal layer in ROP mice (Fig. 2C). The thickness of the outer nuclear layer (ONL) increased significantly in the ROP group; however, the thicknesses of inner-segment/outer-segment (IS/OS) in ROP mice were thinner than those in the control group. The total thicknesses of retinas (from nerve fiber layer (NFL) to RPE) in the ROP model group were greater than in the control group, but this difference was not significant (Fig. 2D).

Hyperoxia-induced formation of autophagosomes

The electron micrographs of retina in ROP model and control mice are showed in Fig. 3. The ultrastructures of retina in control mouse are normal (Fig. 3A). In Oxygen-exposed group, autophagosomes enclosed cytoplasm (Fig. 3B) and bilayer membrane structure (Fig. 3C) were found in retinal cells. Our date indicated that autophagic events are present in the retina of ROP mice.

The effects of hyperoxygen on the autophagy-related gene expressions in ROP model

Analysis of retinal Beclin1, ULK1, and Atg5 mRNA levels revealed time-dependent changes in ROP mice from P8 to P17 (Fig. 4). Expression of Beclin1, ULK1, and Atg5 was upregulated in the hyperoxia phase of ROP relative to the control at P8 to P13. From P14 to P17, in the relative hypoxia phase, the expression of Beclin1, ULK1, and Atg5 mRNA levels was downregulated in the ROP model compare to the controls, and as time passed, the decrease became more and more obvious.

The effects of hyperoxygen on the autophagy and apoptosis-related protein expressions in ROP model

The protein levels of Beclin1 and ULK1 in retinas were upregulated in the relative hypoxia phase (Fig. 5A, B). There was no significant change in the expression of Atg5 between ROP animals and control animals (Fig. 5C). Although the Bax levels in ROP mice increased at first (P8–P9), subsequently the two groups showed no difference; in the relative hypoxia phase, however, the levels of Bax were upregulated again from P14 to P17 (Fig. 5F). In the hyperoxia phase (P8–P11), the protein levels of Bal-2 were upregulated. However, in the relative hypoxia phase (P15–P17), the protein levels of Bal-2 were decreased. Also, the Bcl-2 protein level in the retinas showed a downregulation tendency from P8 to P17 (Fig. 5E). Taken

together, these results indicate that in the retinas of ROP mice, the hyperoxia-induced increase of apoptosis is paralleled by changes in autophagy activation.

Discussion

The development of ROP is accompanied by abnormal proliferation of blood vessels. But in clinical work, after injecting anti-neovascularization drugs in the vitreous cavity, the vision of ROP patients over the long term is still poor. We therefore focused on the changes of autophagy of retinal cells rather than blood vessels. In our research, we observed changes in autophagy markers of retinal cells during hyperoxia (the first stage of ROP; from P8-P12) and relative hypoxia (the second stage of ROP; from P13-P17).

During the hyperoxia phase (P8–P12), the RNA expression of autophagic markers (ULK1, Beclin1, and Atg5) in retina was increased (Fig. 4), which indicates the induction of autophagy in retinal cells. The autophagy events reached a peak in the early phase of the ROP model; initially, the autophagic pathway functions as an adaptive response to stress [13]. We also found that the RNA expression of Beclin1, ULK1, and Atg5 was decreased in the second stage of ROP mice, during the relative hypoxic phase (P14–P17) (Fig. 4). However, changed in protein expression lag behind changed in genes, the protein expression of autophagy (ULK1, Beclin1) increased in retinal cells of ROP mice in the relative hypoxia phase (Fig. 5). This result is in line with the hypothesis that oxidation induced autophagy; meanwhile, autophagy expression is different in different oxygen conditions [9].

ULK1 has been suggested to function in the initial stage of the autophagy pathway. ULK signaling controls autophagosome formation in conjunction with key regulatory factors such as Beclin1 and Atgs. ULK1 was positioned to function upstream of the Beclin1 pathway [14, 15]. In the ROP mice studied here, retinas were characterized by high protein levels of ULK1 from P15 to P17, indicating an induction in the autophagic process of retinas of the ROP model. Moreover, the protein levels of Beclin1 were upregulated from P12 to P17, which means ULK1 may combine with Beclin1 for the multiple autophagy components to form autophagosomes in the retinal cells.

As previously demonstrated, anti-apoptotic Bcl-2 inhabits Beclin 1-dependent autophagy [16]. Under conditions of stress, Bcl-2 is displaced from Beclin1 and Bax to induce autophagy and apoptosis, respectively. In contrast, under conditions of extreme starvation, Bcl-2 is dissociated from Bax, and promotes apoptosis [17]. In the hyperoxia stage of the present study, the stress possibly disrupted the bonding between Bcl-2 and Beclin1 to induce autophagy. In the hypoxia stage, Bax may have promoted caspase-mediated cleavage of Beclin-1, which prevented autophagy and induced apoptosis. The Atg5 cleavage fragment could promote nuclear fragmentation, and cleaved Atg5 directly induces apoptosis but not autophagy.[17] However, in our study, the protein expression of Atg5 showed no significant difference between the hyperoxia phase and the hypoxia phase.

The retina in ROP mice is characterized by reduced autophagy markers at the second stage of relative hypoxia; at that time, cells begin to die [18, 19]. This is in line with our finding that the autophagic expression began to decrease after the mice were removed from the hyperoxic environment. In our study, retinas of the ROP model mice showed edematous changes, the total thicknesses of retinas (from NFL to RPE) in the ROP model group were greater than in the control group, however, their IS/OS layer was thinner than that of control mice at P17, which means the oxygen damaged the structure of the retina. Reduced autophagy is an important pathological feature of ocular diseases [20, 21]. The present results are consistent with the supposition that a reduction in autophagy in ROP mice may result in decreased function of the protective mechanism that is important to retinal cell survival in response to injury.

Previous studies indicated that oxygen-induced retinal apoptosis in a retinopathy model decreased from P13 to P15, then remained constant until P17 [22, 23]. The present results show that in the initial stage of hyperoxia (from P8 to P9) the expression of Bax in retinal cells increased, and then began to decrease (from P10 to P13). From P14 to P17, the expression of Bax increased again. We speculated that the sudden entry into hyperoxic environment led to increased stress response of Bax expression. In addition, the expression of Bcl-2 in retinal cells was upregulated in the hyperoxia phase (from P8 to P11), then decreased in the relative hypoxia phase (P15–P17), and showed a downregulated tendency. These results indicate that in retinas of ROP mice, oxygen-induced increase expression of some apoptotic markers is paralleled by autophagy activation.

In conclusion, the induction of autophagy plays an important role in the pathophysiology of retinal cells in the ROP model. There may be a complex interaction between autophagy and apoptosis that aggravates retinal damage and further impairs visual acuity. Considering the important role of autophagy in ROP, anti-autophagy would have beneficial effects on ROP pathophysiology. However, we still do not fully understand the roles and regulation of autophagy in retinal cells of ROP mice. Which retinal cells play a major role in ROP disease is what we need to further study in the future. At the same time, we need to pay attention to the interaction between autophagy and apoptosis in the pathological process of ROP. Additional studies will help us to determine the potential of autophagy as a therapeutic target for the treatment of human pathologies.

Conclusions

We can conclude that hyperoxia not only cause retinal neovascularization, but also change the autophagy markers in the retina of newborn mice. Our present observations could have impact on the treatment of ROP in the children. Inhibition of autophagic expression in retina could helpful to alleviate the severity of ROP.

Abbreviations

anti-VEGF:anti-vascular endothelial growth factors; Bcl-2:B-cell lymphoma 2; Bax:Bcl-2-associated X protein; H&E:hematoxylin and eosin; IS/OS:inner-segment/outer-segment; NFL:nerve fiber layer; ONL:outer

nuclear layer; PBS:phosphate buffered saline; P7:postnatal day-of-life 7; ROP:retinopathy of prematurity; RPE:retinal pigment epithelial; ULK1:Uncoordinated-51 like kinase 1.

Declarations

Ethics approval and consent to participate

All animal protocols were reviewed and approved by the institutional animal care committee of Zhejiang Chinese Medicine University.

Consent to publish

Not applicable

Availability of data and materials

All date generated and analyzed during this study are included in this article.

Competing interests

The authors declare that they have no competing interests.

Funding

This work was supported by grants from the Natural Science Foundation of Zhejiang Province, (NO. LQ18H120003) to Jie Wang, and (NO: LY19H280011) to Prof. Yunliang Zheng; and Department of Health of Zhejiang Province, (NO.2018KY554) to Jie Wang. The Natural Science Foundation of Zhejiang Province and Department of Health of Zhejiang Province helps us to purchase the reagents and animals needed for the experiment. At the same time, it also will support our subsequent publication charges.

Author's contributions

WJ: Data Collection, Manuscript Preparation, Funds Collection; DE: Statistical Analysis, Literature Search, Manuscript Preparation; ZY: Study Design, Data Interpretation, Manuscript Preparation, Funds Collection. All authors have read and approved the manuscript.

Acknowledgements

The Natural Science Foundation of Zhejiang Province and Department of Health of Zhejiang Province support to this research.

References

1. Hellström A, Smith LE, Dammann O. Retinopathy of prematurity. Lancet. 2013; 382(9902):1445-1457.

2. Tan SM, Stefanovic N, Tan G, Wilkinson-Berka JL, de Haan JB. Lack of the antioxidant glutathione peroxidase-1 (GPx1) exacerbates retinopathy of prematurity in mice. Invest Ophthalmol Vis Sci. 2013; 54(1):555-562.
3. Clark D, Mandal K. Treatment of retinopathy of prematurity. Early Hum Dev. 2008; 84(2):95-99.
4. Åkerblom H, Andreasson S, Larsson E, Holmström G. Photoreceptor Function in School-Aged Children is Affected by Preterm Birth. Transl Vis Sci Technol. 2014; 3(6):7.
5. Hansen RM, Moskowitz A, Akula JD, Fulton AB. The neural retina in retinopathy of prematurity. Prog Retin Eye Res. 2017; 56:32-57.
6. Zhou Z, Doggett TA, Sene A, Apte RS, Ferguson TA. Autophagy supports survival and phototransduction protein levels in rod photoreceptors. Cell Death Differ. 2015; 22(3):488-498.
7. Kuma A, Mizushima N. Physiological role of autophagy as an intracellular recycling system: with an emphasis on nutrient metabolism. Semin Cell Dev Biol 2010; 21: 683–690.
8. Besirli CG, Chinskey ND, Zheng QD, Zacks DN. Autophagy activation in the injured photoreceptor inhibits fas-mediated apoptosis. Invest Ophthalmol Vis Sci. 2011; 52(7):4193-4199.
9. Dehdashtian E, Mehrzadi S, Yousefi B, Hosseinzadeh A, Reiter RJ, Safa M, et al. Diabetic retinopathy pathogenesis and the ameliorating effects of melatonin; involvement of autophagy, inflammation and oxidative stress. Life Sci. 2018; 193: 20-33
10. Smith LE, Wesolowski E, McLellan A, Kostyk SK, D'Amato R, Sullivan R, D'Amore PA.Oxygen-induced retinopathy in the mouse.Invest Ophthalmol Vis Sci. 1994 Jan;35(1):101-111.
11. D'Amato R, Wesolowski E, Smith LE. Microscopic visualization of the retina by angiography with high-molecular-weight fluorescein-labeled dextrans in the mouse. Microvasc Res. 1993; 46(2):135-142.
12. Rabinowitz R, Priel A, Rosner M, Pri-Chen S, Spierer A. Avastin treatment reduces retinal neovascularization in a mouse model of retinopathy of prematurity. Curr Eye Res. 2012; 37(7):624-629.
13. Ouyang L, Shi Z, Zhao S, Wang FT, Zhou TT, Liu B, et al. Programmed cell death pathways in cancer: a review of apoptosis, autophagy and programmed necrosis. Cell Prolif. 2012; 45(6):487-498
14. Chan EY. Regulation and function of uncoordinated-51 like kinase proteins. Antioxid Redox Signal. 2012; 17(5):775-785.
15. Itakura E and Mizushima N. Characterization of autophagosome formation site by a hierarchical analysis of mammalian Atg proteins. Autophagy. 2010; 6: 764-776.
16. Pattingre S, Tassa A, Qu X, Garuti R, Liang XH, Mizushima N, et al. Bcl-2 antiapoptotic proteins inhibit Beclin 1-dependent autophagy. Cell. 2005;122(6):927-939.
17. Mukhopadhyay S, Panda PK, Sinha N, Das DN, Bhutia SK. Autophagy and apoptosis: where do they meet? Apoptosis. 2014; 19(4):555-566.
18. Sennlaub F, Courtois Y, Goureau O. Inducible nitric oxide synthase mediates retinal apoptosis in ischemic proliferative retinopathy. J Neurosci. 2002; 22(10):3987-3993.

19. Narayanan SP, Suwanpradid J, Saul A, Xu Z, Still A, Caldwell RW, et al. Arginase 2 deletion reduces neuro-glial injury and improves retinal function in a model of retinopathy of prematurity. PLoS One. 2011; 6(7):e22460.
20. Boya P, Esteban-Martínez L, Serrano-Puebla A, Gómez-Sintes R, Villarejo-Zori B. Autophagy in the eye: Development, degeneration, and aging. Prog Retin Eye Res. 2016; 55:206-245.
21. Chai P, Ni H, Zhang H, Fan X. The Evolving Functions of Autophagy in Ocular Health: A Double-edged Sword. Int J Biol Sci. 2016; 12(11):1332-1340.
22. Cammalleri M, Locri F, Catalani E, Filippi L, Cervia D, Dal Monte M, et al. The Beta Adrenergic Receptor Blocker Propranolol Counteracts Retinal Dysfunction in a Mouse Model of Oxygen Induced Retinopathy: Restoring the Balance between Apoptosis and Autophagy. Front Cell Neurosci. 2017; 11:395.
23. Casini G, Dal Monte M, Fornaciari I, Filippi L, Bagnoli P. The β-adrenergic system as a possible new target for pharmacologic treatment of neovascular retinal diseases. Prog Retin Eye Res. 2014; 42:103-129.

Figures

Figure 1

Retinal vascular morphology was assessed by angiography. The control mice showed complete peripheral blood vessel growth (A). The oxygen-exposed mice showed severe blood vessel tortuosity (white arrow) and defects in vascular growth from the retinal periphery to the optic disc (red arrow) (B). Neovascular tufts in the peripheral retina. (C). Almost no microvascular perfusion around the optic disc in oxygen-exposed mice (D).

Figure 2

HE staining demonstrates retinal tissue structure Pathological changes of retinal tissues in the retinopathy of prematurity (ROP) group. Retinal structures appear normal in the control group (A). Retinas of ROP model mice show edematous changes, especial the ONL, while the IS/OS layer in the ROP model decreases significantly (B, D). The vessels protrude into the vitreous at the preretinal layer in ROP mice (C, arrows). * $P < 0.05$ between the two groups.

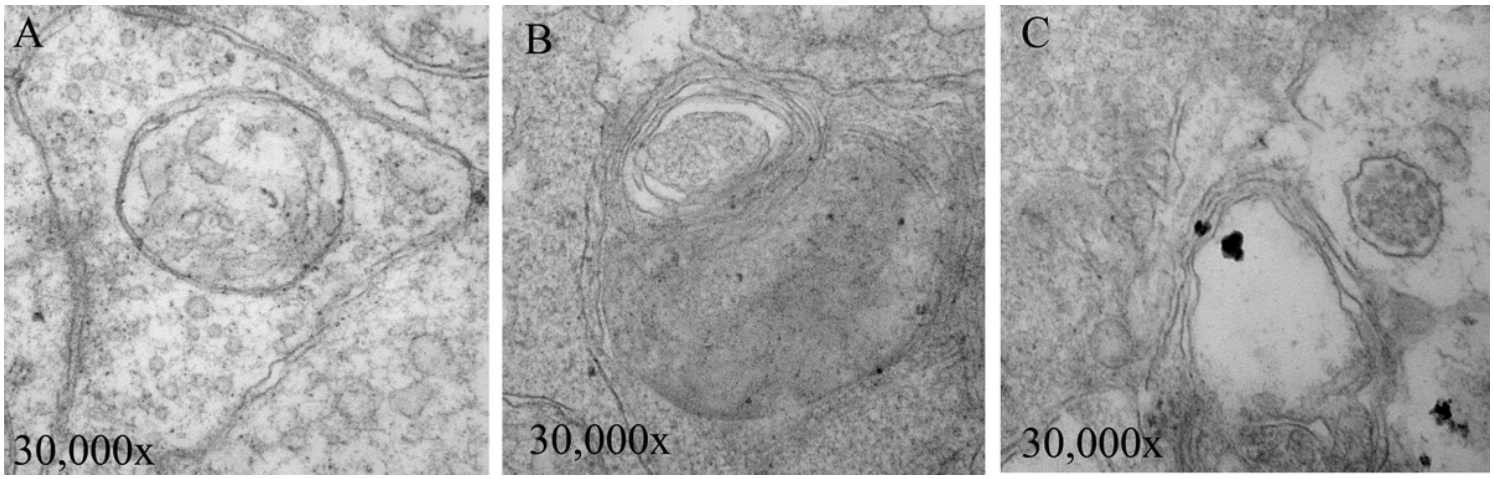

Figure 3

Observation of ultrastructure of retina by electron microscopy Autophagy in the retina of ROP mice at P17: autophagic event were encountered in the mouse retina under electron microscopy. Retinal ultrastructures appear normal in the control group (A). Autophagosomes enclosed cytoplasm (B). Bilayer membrane structure (C).

Figure 4

Beclin1, ULK1, and Atg5 mRNA expression in the retina were evaluated by qPCR Hyperoxia exposure can change Beclin1, ULK1, and Atg5 mRNA expression. Relative gene expression of Beclin1 (A), ULK1 (B), and Atg5 (C) is upregulated in the hyperoxia stage (P8–P13), and downregulated in the relative hypoxia phase (P14–P17). *P < 0.05 compared to the control (room air) group.

Figure 5

Protein levels of autophagy markers, Bal-2 and BAX were evaluated in the retina by Western blot experiments and densitometric analysis. In the relative hypoxia phase (P13-P17), the levels of Beclin-1(A) and ULK1 (B) are upregulated. The level of Atg5 (C) showed no difference between two groups. *P < 0.05 vs. control mice. β-actin was used as the loading control (D). The protein levels of Bal-2 (E) were upregulated from P8 to P11, in the relative hypoxia phase (P15–P17), the protein levels of Bal-2 were decreased. The Bax (F) levels in ROP mice increased at first (P8–P9), subsequently the two groups showed no difference, then the levels of Bax were upregulated again from P14 to P17 *P < 0.05 vs. control mice. β-actin was used as the loading control (G).

Supplementary Files

This is a list of supplementary files associated with this preprint. Click to download.

- NC3RsARRIVEGuidelinesChecklist.pdf